

10-MHz, Yb-fiber chirped-pulse amplifier system with large-scale transmission gratings

Yohei Kobayashi,^{1,4,*} Nozomi Hirayama,^{1,4} Akira Ozawa,^{1,4} Takashi Sukegawa,² Takashi Seki,² Yoshiyuki Kuramoto,² and Shuntaro Watanabe^{3,4}

¹The Institute for Solid State Physics, The University of Tokyo, 5-1-5 Kashiwanoha, Kashiwa, Chiba 277-8581, Japan

²Corporate R&D Headquarters, CANON Inc., Utsunomiya 321-3292, Japan

³Research Institute for Science and Technology, Tokyo University of Science, Noda, Chiba 278-8510, Japan

⁴CREST, Japan Science and Technology Agency (JST), Chiyoda, Tokyo 102-0075, Japan

*yohei@issp.u-tokyo.ac.jp

Abstract: Large-scale transmission gratings were produced for a stretcher and a compressor in the Yb-fiber chirped-pulse amplification system. A 23-W, 200-fs laser system with a 10-MHz repetition rate was demonstrated. Focused intensity as high as 10^{14} W/cm² was achieved, which is high enough for multi-photon processes such as high-order harmonics generation and multi-photon ionization of neutral atoms. High-order harmonics up to 7th order were observed using Xe gas as a nonlinear medium.

©2013 Optical Society of America

OCIS codes: (140.3510) Lasers, fiber; (140.3280) Laser amplifiers; (050.1950) Diffraction gratings.

References and links

1. K. Ishizaka, T. Kiss, T. Yamamoto, Y. Ishida, T. Saitoh, M. Matsunami, R. Eguchi, T. Ohtsuki, A. Kosuge, T. Kanai, M. Nohara, H. Takagi, S. Watanabe, and S. Shin, "Femtosecond core-level photoemission spectroscopy on 1T-TaS₂ using a 60-eV laser source," *Phys. Rev. B* **83**(8), 081104 (2011).
2. K. Okazaki, Y. Ota, Y. Kotani, W. Malaeb, Y. Ishida, T. Shimojima, T. Kiss, S. Watanabe, C.-T. Chen, K. Kihou, C. H. Lee, A. Iyo, H. Eisaki, T. Saito, H. Fukazawa, Y. Kohori, K. Hashimoto, T. Shibauchi, Y. Matsuda, H. Ikeda, H. Miyahara, R. Arita, A. Chainani, and S. Shin, "Octet-Line Node Structure of Superconducting Order Parameter in KFe₂As₂," *Science* **337**(6100), 1314–1317 (2012).
3. A. Cingöz, D. C. Yost, T. K. Allison, A. Ruehl, M. E. Fermann, I. Hartl, and J. Ye, "Direct frequency comb spectroscopy in the extreme ultraviolet," *Nature* **482**(7383), 68–71 (2012).
4. A. Ozawa and Y. Kobayashi, "VUV frequency-comb spectroscopy of atomic xenon," *Phys. Rev. A* **87**(2), 022507 (2013).
5. R. J. Jones, K. D. Moll, M. J. Thorpe, and J. Ye, "Phase-coherent frequency combs in the vacuum ultraviolet via high-harmonic generation inside a femtosecond enhancement cavity," *Phys. Rev. Lett.* **94**(19), 193201 (2005).
6. Ch. Gohle, T. Udem, M. Herrmann, J. Rauschenberger, R. Holzwarth, H. A. Schuessler, F. Krausz, and T. W. Hänsch, "A frequency comb in the extreme ultraviolet," *Nature* **436**(7048), 234–237 (2005).
7. J. Lee, D. R. Carlson, and R. J. Jones, "Optimizing intracavity high harmonic generation for XUV fs frequency combs," *Opt. Express* **19**(23), 23315–23326 (2011).
8. A. Ozawa, J. Rauschenberger, Ch. Gohle, M. Herrmann, D. R. Walker, V. Pervak, A. Fernandez, R. Graf, A. Apolonski, R. Holzwarth, F. Krausz, T. W. Hänsch, and Th. Udem, "High harmonic frequency combs for high resolution spectroscopy," *Phys. Rev. Lett.* **100**(25), 253901 (2008).
9. F. Lindner, W. Stremme, M. G. Schätzel, F. Grasbon, G. G. Paulus, H. Walther, R. Hartmann, and L. Strüder, "High-order harmonic generation at a repetition rate of 100 kHz," *Phys. Rev. A* **68**(1), 013814 (2003).
10. M.-C. Chen, M. R. Gerrity, S. Backus, T. Popmintchev, X. Zhou, P. Arpin, X. Zhang, H. C. Kapteyn, and M. M. Murnane, "Spatially coherent, phase matched, high-order harmonic EUV beams at 50 kHz," *Opt. Express* **17**(20), 17376–17383 (2009).
11. Y. Zaouter, J. Boulet, E. Mottay, and E. Cormier, "Transform-limited 100 microJ, 340 MW pulses from a nonlinear-fiber chirped-pulse amplifier using a mismatched grating stretcher-compressor," *Opt. Lett.* **33**(13), 1527–1529 (2008).
12. J. Boulet, Y. Zaouter, J. Limpert, S. Petit, Y. Mairesse, B. Fabre, J. Higuier, E. Mével, E. Constant, and E. Cormier, "High-order harmonic generation at a megahertz-level repetition rate directly driven by an ytterbium-doped-fiber chirped-pulse amplification system," *Opt. Lett.* **34**(9), 1489–1491 (2009).
13. S. Hädrich, J. Rothhardt, M. Krebs, F. Tavella, A. Willner, J. Limpert, and A. Tünnermann, "High harmonic generation by novel fiber amplifier based sources," *Opt. Express* **18**(19), 20242–20250 (2010).
14. A. Vernaleken, J. Weitenberg, T. Sartorius, P. Russbueldt, W. Schneider, S. L. Stebbings, M. F. Kling, P. Hommelhoff, H. D. Hoffmann, R. Poprawe, F. Krausz, T. W. Hänsch, and Th. Udem, "Single-pass high-harmonic generation at 20.8 MHz repetition rate," *Opt. Lett.* **36**(17), 3428–3430 (2011).

15. T. Eidam, S. Hanf, E. Seise, T. V. Andersen, T. Gabler, C. Wirth, T. Schreiber, J. Limpert, and A. Tünnermann, "Femtosecond fiber CPA system emitting 830 W average output power," *Opt. Lett.* **35**(2), 94–96 (2010).
16. A. Ruehl, A. Marcinkevicius, M. E. Fermann, and I. Hartl, "80 W, 120 fs Yb-fiber frequency comb," *Opt. Lett.* **35**(18), 3015–3017 (2010).
17. D. Yoshitomi, X. Zhou, Y. Kobayashi, H. Takada, and K. Torizuka, "Long-term stable passive synchronization of 50 μ J femtosecond Yb-doped fiber chirped-pulse amplifier with a mode-locked Ti:sapphire laser," *Opt. Express* **18**(25), 26027–26036 (2010).
18. F. Röser, J. Rothhard, B. Ortac, A. Liem, O. Schmidt, T. Schreiber, J. Limpert, and A. Tünnermann, "131 W 220 fs fiber laser system," *Opt. Lett.* **30**(20), 2754–2756 (2005).
19. C. Zhou, T. Seki, T. Sukegawa, T. Kanai, J. Itatani, Y. Kobayashi, and S. Watanabe, "Large-scale high-efficiency transmission grating for terawatt-class Ti:sapphire lasers at 1kHz," *Apex* **4**(7), 072701 (2011).
20. N. Kuse, Y. Nomura, A. Ozawa, M. Kuwata-Gonokami, S. Watanabe, and Y. Kobayashi, "Self-compensation of third-order dispersion for ultrashort pulse generation demonstrated in an Yb fiber oscillator," *Opt. Lett.* **35**(23), 3868–3870 (2010).
21. M. V. Ammosov, N. B. Delone, and V. P. Krainov, "Tunnel ionization of complex atoms and atomic ions by an alternating electromagnetic field," *Sov. Phys. JETP* **64**, 1191–1194 (1986).
22. L. V. Keldysh, "Ionization in the field of a strong electromagnetic wave," *Sov. Phys. JETP* **20**, 1307 (1965).
23. F. H. M. Faisal, "Multiple absorption of laser photons by atoms," *J. Phys. B* **6**(4), L89–L92 (1973).
24. H. R. Reiss, "Effect of an intense electromagnetic field on a weakly bound system," *Phys. Rev. A* **22**(5), 1786–1813 (1980).

1. Introduction

Highly nonlinear processes such as multi-photon absorption, field ionization, and high-harmonics generation (HHG) are usually investigated using a relatively low repetition-rate solid-state laser such as a 1-kHz Ti: sapphire laser or an optical parametric amplifier system. In some applications, higher signal-to-noise-ratios can be obtained with a higher-repetition-rate, high-peak-power femtosecond laser system. For HHG-pumped photo-electron spectroscopy, high repetition-rate pumping is crucial to avoid the space-charge effect of photoelectrons in order to achieve high energy resolution [1, 2]. High-repetition-rate HHG is also applied for vacuum ultraviolet (VUV) optical frequency comb generation. A comb-mode space larger than tens of megahertz is desired for precision measurements [3, 4]. Enhancement cavity technology is utilized for high-repetition-rate HHG to increase the peak intensity [5–8]. However, single-pass HHG is more robust and has some advantages. One can use well-designed and established optics for single-pass HHG such as high-efficiency gas cells, beam guides for phase matching, and optics such as harmonic separators or filters that cannot be used inside an external resonator. HHG can be directly driven with single pass configuration at 100 kHz by a Ti: sapphire laser [9,10] or sub-megahertz repetition rate using an Yb-doped fiber laser system [11–13]. A higher repetition-rate with a larger comb spacing is desired in many applications, such as comb-resolved XUV spectroscopy for investigations of atomic transitions with broader natural line-widths than 1 MHz. Since a focused intensity of more than 10^{13} W/cm² is required for the HHG, 1 μ J pulse energy is necessary assuming a pulse duration of 100 fs and a focused area of 100 μ m². According to the available average power from a femtosecond laser amplifier, a 10-MHz repetition-rate system would be one of the solutions for both high-intensity physics and comb applications. When the system is combined with an enhancement cavity, mJ-level pulse energies can be expected at a 10-MHz repetition rate. Yb-doped lasers are suitable for high repetition-rate and high average power laser systems with short pulse durations because they have large gain bandwidth and high-power laser diodes can be used for the pumping source. Vernaleken et al. demonstrated direct HHG generation driven by a Yb: YAG slab laser system [14]. An Yb-fiber laser system is advantageous in obtaining short pulse durations compared with other Yb-doped material, but has the disadvantage of high peak power inside the fiber. In a fiber amplifier, the beam propagates in a small core so that nonlinear effects such as self-phase modulation tend to occur. Since the available core size with single-transverse-mode operation is limited, the pulse duration in an amplifier has to be stretched enough to avoid possible nonlinearities. The usual reflection-type grating with a metal coating is not suitable because the thermal expansion effect degrades the beam quality with high average power. In addition, the diffraction efficiency of a metal-coated grating gradually decreases in long-term operation.

The dielectric-coated grating is often used for the high-power system in Nd: glass lasers or Yb-fiber lasers [15], but has a small diffractive bandwidth for the ultra-short pulse generation. A transmission grating has a high damage threshold and wide bandwidth with high diffraction efficiency. It can be used at an exact Littrow angle for the maximum efficiency, and is thus widely used for Yb-fiber laser systems [12, 16–18]. There are 100 W, femtosecond fiber laser systems that have been realized with high repetition rates approximately 100 MHz. The large transmission gratings for these setups are sometimes made using soft materials such as polymers, and therefore the beam size has to be large enough on the grating to avoid overheating or damage. The typical compressor efficiencies with transmission gratings in previous experiments were limited to the range of ~50% to ~80%. A large-scale, high-efficiency, and high-damage-threshold grating was developed and recently applied for a Ti: sapphire chirped-pulse amplifier (CPA) system [19]. The development of a larger-scale transmission grating for a femtosecond Yb-fiber laser system at the 1 μm wavelength region has been desired for a high-intensity laser system with a high repetition-rate which produces very high-average power. Then the heat-resistance property of the transmission grating made of fused silica is crucial. The target stretched pulse duration is 500 ps to avoid the nonlinear phase shift considering the B-integral value in a fiber. Therefore a sufficiently large grating to handle 500 ps pulses (full-width half-maximum) should be developed.

In this paper, we have designed and developed 180 mm-wide fused-silica transmission gratings for a Yb-doped fiber laser CPA system. A diffraction efficiency of 96% was achieved, leading to a 85% throughput of the compressor, which is the highest efficiency in a high-power Yb-fiber system with a transmission grating compressor to the best of our knowledge. The Yb-fiber CPA system with these gratings both in a stretcher and a compressor produced an average of 23 W of power with a pulse duration of 200 fs at a 10-MHz repetition-rate with negligible nonlinear phase shift because of the long stretched pulse duration. The peak power was 10 MW, and the laser was focused into an almost diffraction-limited spot. A focused intensity of 10^{14} W/cm² was realized which was high enough for the HHG. A single-pass HHG up to the 7th harmonic was observed using Xe gas as the nonlinear medium. The multi-photon ionization of neutral atoms was also investigated. Ion currents of Xe and Kr were observed with high signal-to-noise ratio thanks to the high repetition-rate measurement. The obtained ionization probabilities were in good agreement with the theoretical curves of the field ionization.

2. Laser system

The schematic of the laser system is shown in Fig. 1. The oscillator is a Yb-fiber mode-locked laser using a typical configuration of the nonlinear polarization rotation method [20]. The main difference between this system and a conventional oscillator is the low repetition rate. A 20-m single-mode fiber (SMF) is connected to a gain fiber with a 1200 dB/m pump absorption for operation at 10 MHz. The large amount of dispersion due to long fiber is compensated by a grating pair with 1200 lines/mm. The residual higher-order dispersion could be a possible issue of this low repetition-rate oscillator. The grating pair in the oscillator compensates the group-delay dispersion (GDD), while introducing huge third-order dispersion (TOD) in addition to the TOD caused by a long SMF. Therefore, the residual chirp in one round trip is larger compared to a conventional higher repetition-rate oscillator. This issue simply makes the output spectrum narrower compared to the conventional high-rep laser. As a result, the stable mode-locked operation was realized despite the above issues. The output power is approximately 3 mW with the transform-limited pulse duration of 150 fs. The mode-locking could be maintained for months.

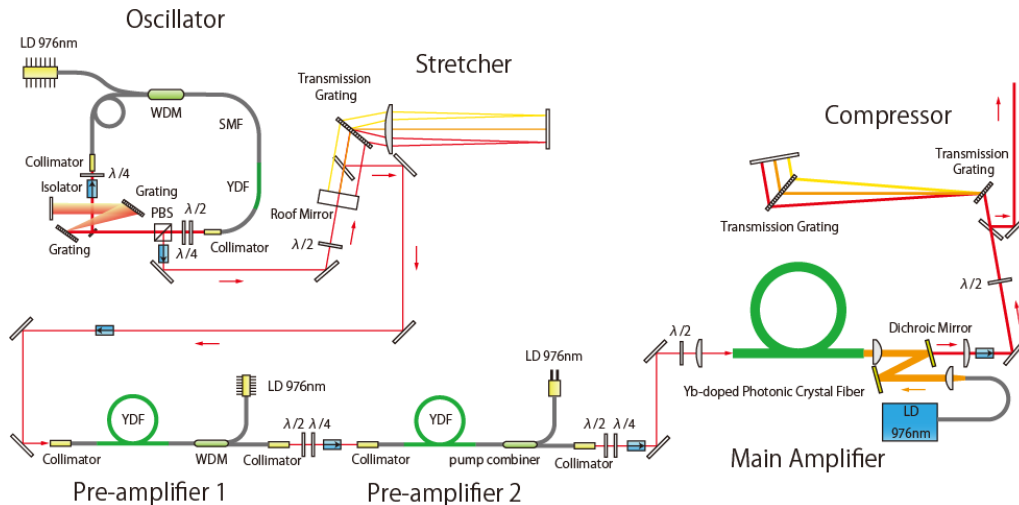


Fig. 1. Schematic of the experimental setup. WDM, wavelength division multiplexer; PBS, polarized beam splitter; SMF, single-mode fiber; LD, laser diode; $\lambda/2$, half waveplate; $\lambda/4$, quarter waveplate; YDF, Yb-doped fiber. Blue boxes with arrows are isolators.

As described in the previous section, a sub-nanosecond pulse stretch is necessary for multi micro-joule pulse generation in a single-mode fiber amplifier. A 180-mm wide and 40-mm high transmission grating with a groove density of 1250 lines/mm was developed (CANON). The grating was fabricated by an etching process on a 1-mm thick fused-silica substrate, and the back surface had an anti-reflection coating. A micrograph of the fabricated grating surface is shown in Fig. 2(a). The grating is a laminar type, and the line depth and the duty cycle are 1.45 μm and 45%, respectively. Figure 2(b) shows the calculated diffraction efficiency of the line depth and the duty cycle assuming a single optical frequency of 1030 nm. The expected maximum efficiency is 97.2% with this groove density. Figure 2(c) shows the measured diffraction efficiency at various incident angles using a broad-band mode-locked oscillator as a test light. The spectrum of this test beam covers from 1020 to 1090 nm, which is shown inset of Fig. 2(c). The diffraction efficiency was measured with a grating-compressor configuration. The total throughput was measured while changing the incident angle and the diffraction efficiency was calculated. The obtained diffraction efficiency was 95.3% at an incident angle of 40 degrees, which corresponds to the Littrow angle. The maximum diffraction efficiency was obtained when the polarization of the incident light is parallel to the lines in the grating (TE), while it decreases to 40% when the polarization is rotated 90 degrees (TM). The measured diffraction efficiency was slightly lower than the estimated value because of the wide spectrum of the test light. With the narrower band spectrum of the 10-MHz laser system, the total throughput efficiency of the compressor was observed to be 85.2%, corresponding to a 96.1% diffraction efficiency in each grating. The stretcher was a conventional Martinez type consisting of a 180 mm transmission grating and an $f = 1000$ mm lens with a diameter of 150 mm. The distance from the grating to the lens was 250 mm, so that the applied GDD was $1.6 \times 10^7 \text{ fs}^2$. The total throughput of the stretcher was 65.4% because of numerous reflections on the metal-coated mirrors in the stretcher. The pulse was stretched to 500 ps in full-width half-maximum with the average power of 2 mW. The actual temporal pulse shape after the stretcher was observed by a fast photo detector and a sampling oscilloscope as shown in Fig. 3. The original spectrum from the oscillator had some peaks in both shorter and longer wavelength edges, and peaks at the shorter wavelength region disappeared at the stretcher because of the geometric restriction as shown in Fig. 3(a). This characteristic spectral shape can be found in the temporal shape. Since the stretcher adds the positive chirp on the almost-transform limited pulse, the longer wavelength part with some peaks in the spectrum appears at the leading edge of the pulse in temporal domain as shown

in Fig. 3(b). The measurement shows a clear chirp added by the stretcher, leading to the pulse duration of 0.5 ns.

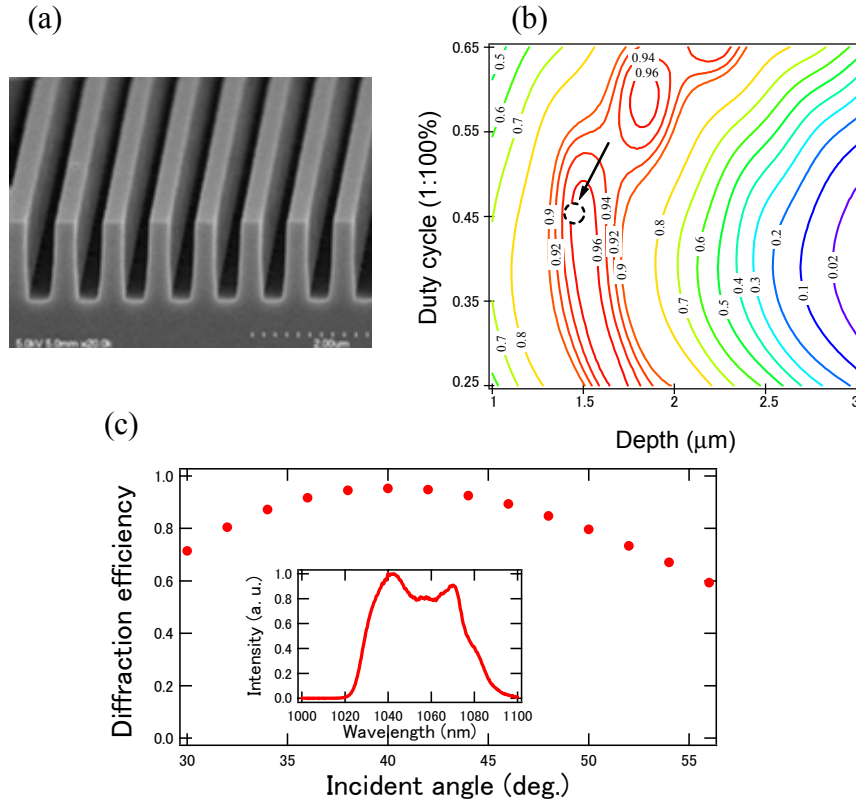


Fig. 2. (a) A micrograph of the surface of the grating. The line depth is $1.4 \mu\text{m}$ with a duty cycle of 0.45. (b) Calculated diffraction efficiency for various duty cycles and line depths. The dotted circle shows the parameters for the manufactured grating. (c) Measured diffraction efficiency of the transmission grating with various incident angles. Inset shows the optical spectrum used for this measurement.

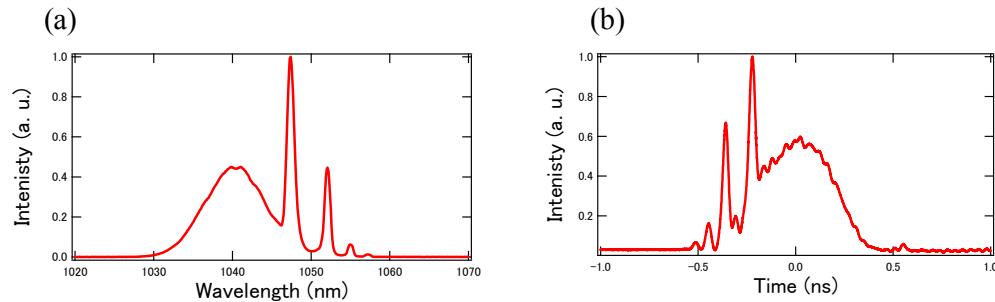


Fig. 3. (a) The spectrum after the stretcher. (b) The temporal pulse shape observed by a fast photo diode. The stretched pulse shape shows a clear chirp, whose structure corresponds to the spectral shape. The stretched pulse duration is 0.5 ns.

The stretched pulse is amplified by two successive Yb-fiber pre-amplifiers. The first amplifier consisted of a $6 \mu\text{m}$ core, 30 cm Yb-doped fiber with an absorption coefficient of 1200 dB/m and a wavelength division multiplexer to combine a pump beam. A 976-nm SMF-coupled wavelength-stabilized pumped laser diode is used for the pump source. With a pump

power approximately 200 mW, a seed beam of 2 mW is amplified to 30 mW. The amplified beam is collimated and coupled into an isolator and then the second amplifier. For the second amplifier, a 3-m double-clad Yb-doped fiber with a 10- μm core and 125- μm first cladding was utilized. The pumping source was a multi-mode fiber-coupled 976-nm laser diode with 5 W power. The pump beam was coupled into the first cladding of the double-clad active fiber by using a pump combiner, while a seeding beam was coupled into the core through a SMF. The pump beam was absorbed by the Yb ions in the core propagating through the first cladding. When the pump power was 2.4 W, the amplified output power was 0.7 W. Backward pumping was adopted in both preamplifiers. Optical isolators were inserted between each of the optical components, as shown in Fig. 1. In the power amplifier, a 1.2-m, polarization-maintaining photonic-crystal fiber was used with the mode diameter of 30 μm (NKT photonics). The pumping source was a 400- μm -core fiber-coupled, 70-W laser diode with a wavelength of 976 nm. The pump beam was collimated and focused into the first cladding using two aspheric lenses after a double bounce of dichroic mirrors to prevent the amplified beam entering the pump laser. The amplified beam was passed through the dichroic mirror and was collimated by a lens. The output power behind the optical isolator was 27.2 W with a pumping power of 54 W. Owing to the large stretcher with a high pulse-stretching factor, the designed intensity inside the gain fiber of the main amplifier was maintained at less than 1 GW/cm². The B-integral for the whole system is estimated to be less than 1 rad.

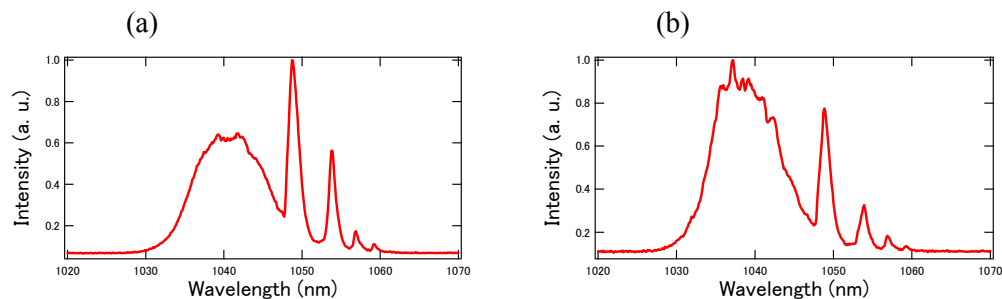


Fig. 4. Optical spectra measured after the (a) preamplifier, and (b) main amplifier.

Figure 4 shows spectra measured after (a) the pre-amplifier and (b) the main amplifier. A slight gain-narrowing effect can be seen in the spectrum after the power amplifier. No obvious spectrum modulation due to the nonlinear effect was observed after the amplifier. The same transmission gratings were used for the pulse compressor. The total throughput of the compressor was 85.2%. Although the average power in the compressor is very high with a relatively small beam size of approximately 3 mm, no damage to the compressor grating or degradation in the efficiency was observed over a one-year period of operation. The grating separation was approximately 1.5 m. The average power of the compressed pulse was 23.2 W. The temporal profile of the compressed pulse was investigated with the second-harmonic generation frequency-resolved optical gating (FROG) method. The observed pulse trace is shown in Fig. 5. There is no pedestal in the temporal pulse shape. The pulse duration was 200 fs with an almost flat spectral phase. No obvious FROG-trace change was observed when the output power was changed from 3 to 23 W with fixed grating separation. This also guarantees the absence of the nonlinear phase shift in the fiber amplifier. After the main amplifier, a pulse energy of 2.3 μJ was obtained and the corresponding peak power was calculated to be 10 MW. Since the fiber laser system has good spatial beam quality, the diffraction-limited focusing can be easily realized by using single aspheric lenses. Assuming a focused beam area of 10 μm^2 , a peak intensity of 1×10^{14} W/cm² should be obtained, which is high enough for the multi-photon ionization of neutral atoms.

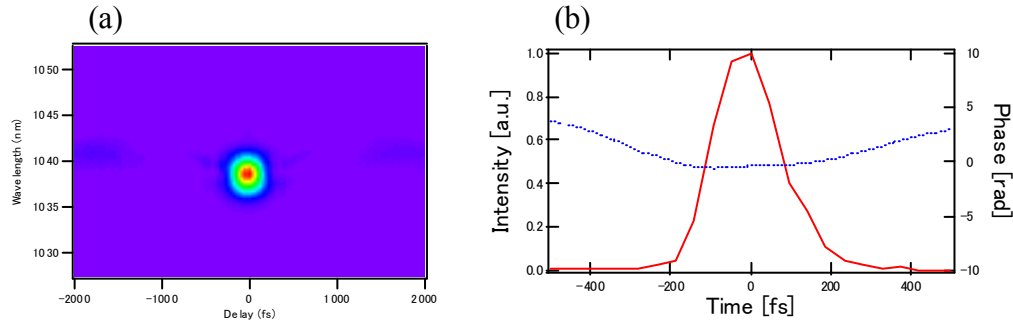


Fig. 5. (a) Observed FROG-trace with an average power of 23 W. (b) Retrieved temporal pulse shape and phase. This shows a pulse duration of 200 fs with no obvious pedestals.

3. Multi-photon ionization

It is crucial to measure the focused intensity of the laser pulse using the photo-ionization process since the auto-correlation or FROG methods sometimes overestimate the peak intensity owing to their low-order nonlinearity. It is one of the well-established methods to estimate the intensity by fitting the experimental data to the theory of field ionization. Since the photo-ionization is strongly intensity-dependent, the peak intensity can be characterized accurately using this method [21–24]. The experiment of multi-photon ionization using a 10-MHz laser system is also significant as a demonstration of high-field physics with high S/N at a high repetition-rate. It was attempted to observe an ion current produced by the multi-photon ionization of Xe and Kr. The compressed pulse was tightly focused by a $f = 15$ mm aspheric lens. At the focus, the spatial beam profile is imaged onto the CCD, and the intensity FWHM of the focused field was found to be approximately $3 \mu\text{m}$. The estimated intensity was approximately 10^{14} W/cm^2 , which is high enough to generate Xe and Kr ions by multi-photon ionization. First, observation of a Xe plasma in air at atmospheric pressure was tested. Xe gas was supplied from a $100\text{-}\mu\text{m}$ diameter hole in a glass tube with a backing pressure of 3 atm at the focus, and a plasma emission from Xe gas was observed by eye. A vacuum chamber was constructed in order to observe the ion current and quantify the multi-photon ionization. The ion current was measured using two electrodes with approximately a 1-mm gap placed at the focal point. A 27-V bias voltage was applied between the electrodes. Scanning the laser power using a half-wave-plate and a polarizer after the amplifier, the electric current was measured with a $1\text{-M}\Omega$ load resistance. The converted voltage was obtained using a digital multimeter (Agilent: 34410A), and the data recorded by a PC. The result is shown in Fig. 6. The ion current of Xe gas as a function of laser intensity is plotted in Fig. 6(a). A signal-to-noise ratio of more than 6 orders of magnitude was obtained because of several reasons, as follows. First, when the laser and measurement system is affected by external perturbation such as mechanical vibration and thermal fluctuation that has typical noise frequency lower than the pulse repetition frequency, resulting signal averages faster with higher repetition rate system that has many sampling points within the characteristic time-scale of noise. Therefore better SN ratio can be obtained with higher repetition rate measurement. Second, the total signal increases with a higher average-power laser compared with the low-repetition laser system, that eliminates the contribution from the shot noise and improves the SN ratio. The obtained data was fitted with the theoretical curve for tunneling ionization probability. Strictly, multi-photon ionization theory should be employed to reproduce the ion current measurement of Xe gas; however, reasonable agreement with the measurement is obtained within a factor of three in the peak intensity when the tunneling ionization probability is used [21]. The ion current measurements for Kr are shown in Fig. 6(b). For Kr gas, the tunneling theory can be adopted more accurately, and the curve fitting results in the intensity shift of only 1.2 between the data and the theory. The tunneling or

multi-photon ionization experiments were performed using a 10-Hz or a 1-kHz repetition-rate laser. The repetition-rate increased by four orders of magnitude, and therefore the signal-to-noise ratio improved significantly. The absolute value of the obtained ion current was also in good agreement with the estimated value from the ionization probability and the gas density.

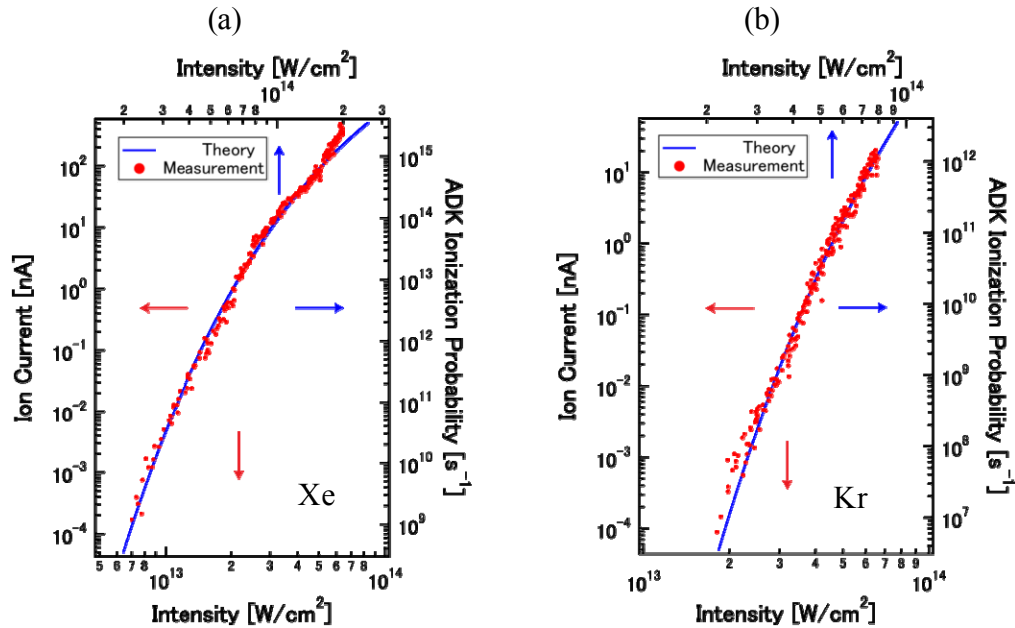


Fig. 6. Ion current measurement of Xe (a) and Kr (b). The bottom x-axes show the estimated intensity from the experiment, and the top x-axes show the fitted intensity to the tunneling ionization probability. The left y-axes show the observed ion current, and the right y-axes show the ionization probabilities.

4. High harmonic generation

In order to observe the HHG with this laser system, the laser beam was focused by a $f = 15$ mm lens, and Xe gas was supplied at the focal point with backing pressure of 3bar. The glass capillary with $\sim 150\mu m$ of opening diameter is used as a gas nozzle. The incident beam size into the chamber was approximately three times smaller compared with the previous experiment and the focal radius is estimated to be about $7\mu m$ (FWHM). The focused intensity is about $1 \times 10^{13} W/cm^2$. A looser focus compared to the previous experiment would be better to generate higher-power, low-order harmonics because of the longer Rayleigh length, which realizes a better phase matching condition. The generated harmonics were separated from the fundamental beam using a MgO Brewster plate, which transmitted the fundamental beam while the HHG is reflected by a Fresnel reflection. The reflected HHG was collimated by a concave mirror with a radius of 80 mm and spectrally resolved by a 1200-lines/mm grating. A photomultiplier tube (PMT) with a MgF_2 window was placed after a slit, and the photo-current from the PMT was measured. The detected wavelength region was limited by a photocathode material and the transmission of the window with a range of 120–400 nm. Rotating the grating angle, the photo-current was measured (Fig. 7). An Xe plasma emission at around 170 nm and 3rd, 5th, and 7th harmonics are clearly observed. Higher harmonics could not be detected by this home-made spectrometer because of the window of the PMT.

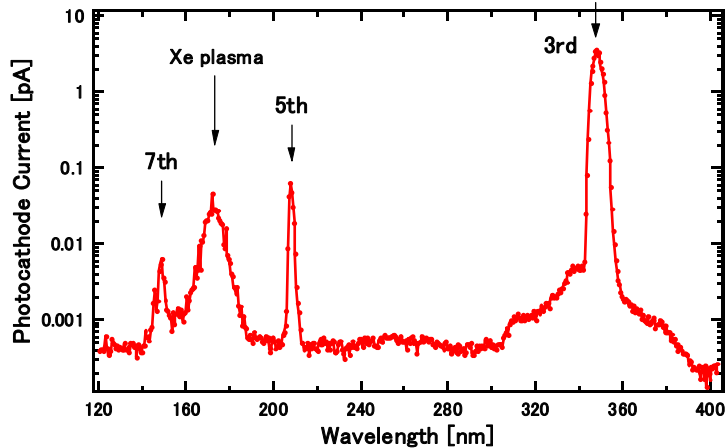


Fig. 7. The 3rd, 5th, and 7th harmonic spectrum generated by Xe gas. Plasma emission around 170 nm is also observed. Higher harmonics were absorbed by the window of the detector.

5. Conclusion

A high intensity laser system with a 10-MHz repetition-rate was developed with the help of a large-scale transmission grating. The laser system was used under the conditions of 10 MW and 200 fs to investigate highly nonlinear phenomena such as multi-photon ionization of rare gases and the high-order harmonic generation. This laser system could be stabilized to an optical frequency comb so that precision spectroscopy and high-intensity physics could be merged. Although the stretcher and compressor systems are relatively large in size, the entire system was found to be stable both in beam direction and output power over long periods of time. No degradation in the compressor efficiency was observed when operated for one year. The generated HHG power from this laser system is still too weak to apply it to photoelectron spectroscopy. A higher HHG power could be achieved by improving the laser system with larger mode-area photonic crystal fibers as a gain medium, which could generate a 100-W average power.

Acknowledgment

This research was supported by the Photon Frontier Network Program of the Ministry of Education, Culture, Sports, Science and Technology, Japan.